ELSEVIER

Journal of Structural Geology 29 (2007) 1445–1462

JOURNAL OF STRUCTURAL GEOLOGY

www.elsevier.com/locate/jsg

Vein quartz microfabrics indicating progressive evolution of fractures into cavities during postseismic creep in the middle crust

Jens-Alexander Nüchter*, Bernhard Stöckhert

Institut für Geologie, Mineralogie und Geophysik, Ruhr-Universität Bochum, Universitätsstrasse 150, D-44721 Bochum, Germany

Received 20 March 2007; received in revised form 12 July 2007; accepted 17 July 2007
Available online 27 July 2007

Abstract

Discordant quartz veins in metamorphic rocks formed at temperatures similar to 300 °C in an extensional tectonic regime. The vein shape is characterized by an aperture to length ratio exceeding the maximum value feasible for purely elastic deformation by orders of magnitude. Non-elastic ductile deformation of the host rock must have controlled widening of the arrested cracks. Fracture parallel shortening is low. Due to the low accumulated strain, the microstructural record of this stage of deformation cannot be isolated in the polyphase host rock. Information is exclusively obtained from the microfabrics of the vein sealing quartz. There, the density of geometrically necessary dislocations, derived from orientation maps created by electron backscatter diffractometry (EBSD), decreases markedly from the vein wall to the centre. The gradient is attributed to progressive cavity formation and buckling of the vein walls during sealing. Early grown crystals at the vein margins record a prolonged deformation history compared to lately grown grains in the centre of the vein. The gradient and the lack of significant crystal plastic deformation of the crystals in the vein centre show that deformation of the completed vein is insignificant compared to deformation during progressive opening and sealing. In view of the precursory brittle deformation and the intense crystal plastic deformation at the vein margins, the monogenetic veins are interpreted to record a single mid-crustal stress transient, related to the earthquake cycle. Fracturing is proposed to be a consequence of coseismic loading, while progressive opening and sealing record the deformation during postseismic stress relaxation by creep.

Keywords: Postseismic stress relaxation; Brittle/ductile deformation; Veins; Seismic cycle

1. Introduction

Exhumed metamorphic rocks provide insight into processes and conditions at deeper levels of the crust, which are not accessible to direct observation with any comparable resolution and detail by geophysical methods. For instance, the effects of seismicity in the upper crust on stress changes and transient deformation in the middle and lower crust are poorly understood so far. Upon exhumation, originally deep-seated crust composed of metamorphic rocks has to pass the brittle–ductile transition zone (BDT). Approaching the BDT from below in a tectonically active region means that the rocks get more and more affected by cyclic stress changes related to seismic activity in the overlying seismogenic layer (schizosphere sensu Scholz, 1990). Numerical models show that a crustal volume in the plastosphere, beneath the tip of a seismically active fault, is loaded to high stress during major earthquakes (Ellis and Stöckhert, 2004a,b). These stresses are relaxed during a subsequent episode of viscous postseismic creep that contributes to postseismic deformation recorded at the surface by modern geodetic techniques (e.g. Pollitz et al., 2001; Freed and Bürgmann, 2004; Freed et al., 2006; Ellis et al., 2006). Metamorphic rocks that have passed upwards through the uppermost plastosphere in an active tectonic environment are expected to bear the record of such stress cycles. The structures and fabrics reflecting coseismic loading and postseismic stress relaxation should bear the characteristics of episodic non-steady state deformation.

* Corresponding author. Tel.: +49 234 32 23 235; fax: +49 234 32 14 572.
E-mail address: jens.nuechter@rub.de (J.-A. Nüchter).

0191-8141/$ - see front matter © 2007 Elsevier Ltd. All rights reserved.
doi:10.1016/j.jsg.2007.07.011

Previous reports on the record of seismically induced stress cycles in rocks once situated in the middle crust focused on microstructural features. These comprise fabrics indicating localized crystal plastic deformation at high stress (Trepmann and Stöckhert, 2001, 2003) or brittle failure (Mullis, 1975; Küster and Stöckhert, 1999; Trepmann and Stöckhert, 2002), followed by creep at decreasing stress. In the present paper, we investigate what is suspected to be the record of the seismic cycle on the mesoscopic scale. The objective is distributed episodic deformation in an extensive volume of middle crust in the vicinity of a seismogenic fault in the formerly overlying schizosphere, not that of localized deformation within a shear zone extending downwards from the fault. Lenticular quartz veins, discordant with respect to all syn-metamorphic structures, are widespread in high pressure–low temperature metamorphic rocks of the Styra-Och Unit in the south of Evia Island (Greece). The fabrics and the geometry of these veins are interpreted to record such episodic deformation in the uppermost plastosphere at temperatures near to or somewhat above 300 °C. The structural record indicates that tensile failure was followed by a stage of ductile deformation to low finite strain.

The veins in the Styra-Ochi Unit formed from cracks, which widened to create space for mineral precipitation from the crack-filling fluid. For cracks of limited length, the widening of the crack and formation of a lens-shaped cavity implies shortening of the host rock parallel to the crack. The amount of elastic distortion is limited by the elastic properties and the tensile strength of the host rock. Crack opening by purely elastic deformation is therefore restricted to high crack aspect ratios (here aspect ratio denotes the ratio length/width). In the case of veins with a low aspect ratio, there must be a contribution of non-elastic deformation of the host rock, as predicted by a linear elastic fracture mechanic (LEFM) approach (e.g. Sneddon and Elliott, 1946; Pollard and Segall, 1987; Vermilye and Scholz, 1995; Olson, 2003). At elevated temperatures, this non-elastic deformation is expected to be time-dependent and concomitant to stress relaxation.

The microstructural record of this stage of ductile deformation cannot be isolated in the host rock, the microstructure of the polyphase material being too complex and strain too low. Information can be obtained from the vein quartz, however. On principle, the precipitation of quartz in the cavity could have occurred either in a static environment, after formation of the cavity, or during progressive time-dependent opening. To discriminate between these end-members, here we investigate the microfabrics of the vein quartz as a function of position in the vein.

At first, we show that the apertures of the veins in southern Evia systematically exceed the maximum value predicted by LEFM analysis for the given fracture length. Then, the microfabrics of the vein quartz are investigated to test whether crystallization took place in a static environment or during progressive widening of the cavity, controlled by viscous creep of the host rock. While elastic distortion of the host rock is instantaneous in response to loading by remote stress, ductile creep is time-dependent and slow compared to elastic distortion. It depends on host rock rheology and ambient conditions. This means that cracks, which opened by quasi-instantaneous purely elastic distortion of the host rock get sealed in a static environment, whereas cracks opening by viscous creep can get sealed during progressive opening. If so, early grown grains at the vein walls record a prolonged deformation history compared to lately grown grains. Also, if crack opening takes place by creep during stress relaxation after an event of rapid loading, the early grown crystals would be subject to higher stresses compared to those grown lately in the centre of the vein. A gradient in the style and intensity of crystal plastic deformation, decreasing inwards from the vein walls and reflecting a history, is expected. Finally, we show that the predominant portion of crystal plastic distortion of the vein quartz was accumulated during progressive cavity opening and sealing, while later overprint on the completed vein is insignificant. This implies that the discordant veins in the Styra-Ochi Unit are the result of a stage of transient and episodic deformation. The objective of the present paper is to test the hypothesis, that the veins record an event of rapid loading, presumably driven by stress redistribution during a nearby seismic event, and subsequent stress relaxation by creep of the host rock with precipitation of minerals from the pore fluid in the progressively widening cavity.

2. Geological setting

The Styra-Ochi Unit in southern Evia Island, Greece, is part of the high pressure/low temperature (HP/LT) metamorphic internal Cyclades belt, situated in the backarc region of the active Hellenic subduction zone. The structure of the Cyclades is governed by extensional tectonics and crustal thinning since the Early Miocene (Le Pichon and Angelier, 1981; Jolivet and Faccenna, 2000), driven by continuing roll back of the Hellenic subduction zone (Meulenkamp et al., 1988). The extension is localized in a single major (Lister et al., 1984; Faure et al., 1991) or several (Gautier and Brun, 1994) detachment faults. Southern Evia represents the footwall block to a detachment fault, while remnants of the hanging wall block are preserved on the neighbouring islands of Tinos, Kea, and Paros (Gautier and Brun, 1994).

The HP/LT metamorphic Styra-Ochi Unit in southern Evia is derived from a variety of siliciclastic and carbonate-rich marine sediments, with intercalated basaltic to rhyolitic volcanic and intrusive rocks (Fig. 1). During its earlier history, the Styra-Ochi Unit underwent pervasive deformation and HP/LT metamorphic overprint at a maximum temperature of about 400 °C and a pressure similar to 1 GPa (Klein-Helmkamp, 1996), indicating maximum burial to a depth of about 30–35 km. It was exhumed as a coherent unit, interpreted to represent the footwall block of a metamorphic core complex. The structures developed during that stage reflect a continuous evolution from ductile to brittle extensional deformation within a uniform kinematic framework (Fig. 1) (Gautier and Brun, 1994; Klein-Helmkamp, 1996). The veins investigated in the present study formed during exhumation and postdate HP/LT metamorphism.

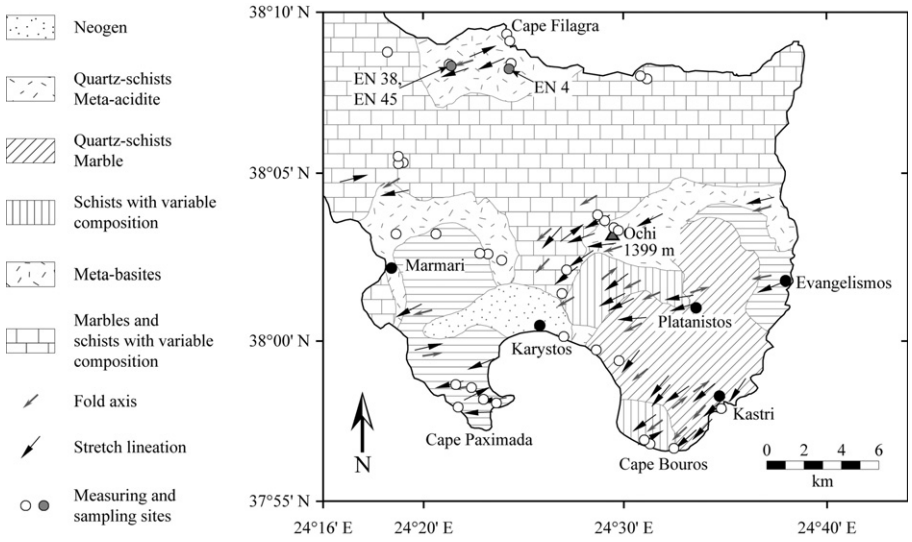

Fig. 1. Geological map of southern Evia, modified after Jacobshagen (1986), with structural information from Klein-Helmkamp (1996). The measurement and sampling sites are indicated.

3. Methods

Length and aperture of 79 discordant quartz veins were measured in the field. The sites are plotted in a geological map (Fig. 1). A correction was applied in those cases, where the angle between the outcrop surface and the vein wall deviates significantly from 90°. Oriented samples were taken from 33 veins. Additionally, 3 veins were sampled along profiles normal to the vein walls (Fig. 1): (1) a vein corresponding to vein EN 4 (Fig. 2a); (2) vein EN 38 (Fig. 2b); (3) EN 45 (Fig. 2c). The samples are cut normal to the host rock foliation and normal to the vein wall. The microstructures were examined in thin section (30 μm thick) with a polarizing microscope. The scanning electron microscope (SEM)-based technique of electron backscatter diffraction (EBSD), using polished thin sections, yields microstructural information with a resolution on the micrometre scale and provides information on the spatial distribution of the full crystallographic orientation in a thin section. EBSD-investigations were carried out using an SEM (LEO 1530) equipped with a field emission gun and a forescatter detector. Thin sections used for the EBSD technique were chemically polished using a silica suspension (SYTON®) to minimise surface damage, and then coated with carbon to limit charging effects. For EBSD analysis, the SEM was operated at an accelerating voltage of 20 kV and a working distance of 25 mm, with the thin section tilted at an angle of 70° with respect to the beam.

4. Structural setting of the quartz veins

The veins of interest crosscut all former syn-metamorphic structures and fabrics, including schistosity (Figs. 2a–c, 3), folds, and earlier veins parallel to the foliation (Fig. 2b). Most veins are symmetrically lenticular (Fig. 2a, b), while a few veins are more irregular in shape (Fig. 2c). Displacement parallel to the vein walls is not observed (Fig. 2b). The geometry suggests tensile failure (mode I) and opening normal to the least principal stress, σ_3. The orientation of the vein walls, hence of the original cracks, is more or less uniform all over the Styra-Ochi Unit in southern Evia, an area of more than 500 km^2. The veins strike SE to SSE and are nearly vertical. This orientation is consistent with a stress field characterized by $\sigma_1 = \sigma_v$ and σ_3 trending NE to ENE at the stages of fracturing and vein formation (Fig. 3). The length of most veins ranges between 10^{-1} m and 10^{1} m, which is taken to reflect the characteristic length scale of the parental cracks. The spectrum of vein aspect ratios ranges between 7 and 100 (Fig. 4). Sixty-two per cent of the veins show aspect ratios <20 (Fig. 4).

5. Vein geometry in the context of linear elastic fracture mechanics

In response to linear elastic deformation of the host rock, opening of an arrested crack is controlled by the elastic properties of the host rock (e.g. Sneddon and Elliott, 1946; Pollard and Segall, 1987; Vermilye and Scholz, 1995; Olson, 2003) and the effective stress acting normal to the crack wall, $\sigma'_n = \sigma_n - P_f$ (Rice and Cleary, 1976). σ_n denotes the remote stress component acting normal to the crack wall, in this case the least principal compressive stress σ_3, and P_f denotes the fluid pressure inside the crack. In the following, compressive stresses are denoted by positive values and tensile stresses by negative values, as commonplace in structural geology.

Linear elastic fracture mechanics (LEFM) predicts that the aperture w of an arrested crack correlates with the crack length L and with the wall normal effective tensile stress σ'_n. The following relation holds for non-interacting, opening mode cracks under two-dimensional plane strain conditions (Sneddon and Elliott, 1946; Pollard and Segall, 1987):

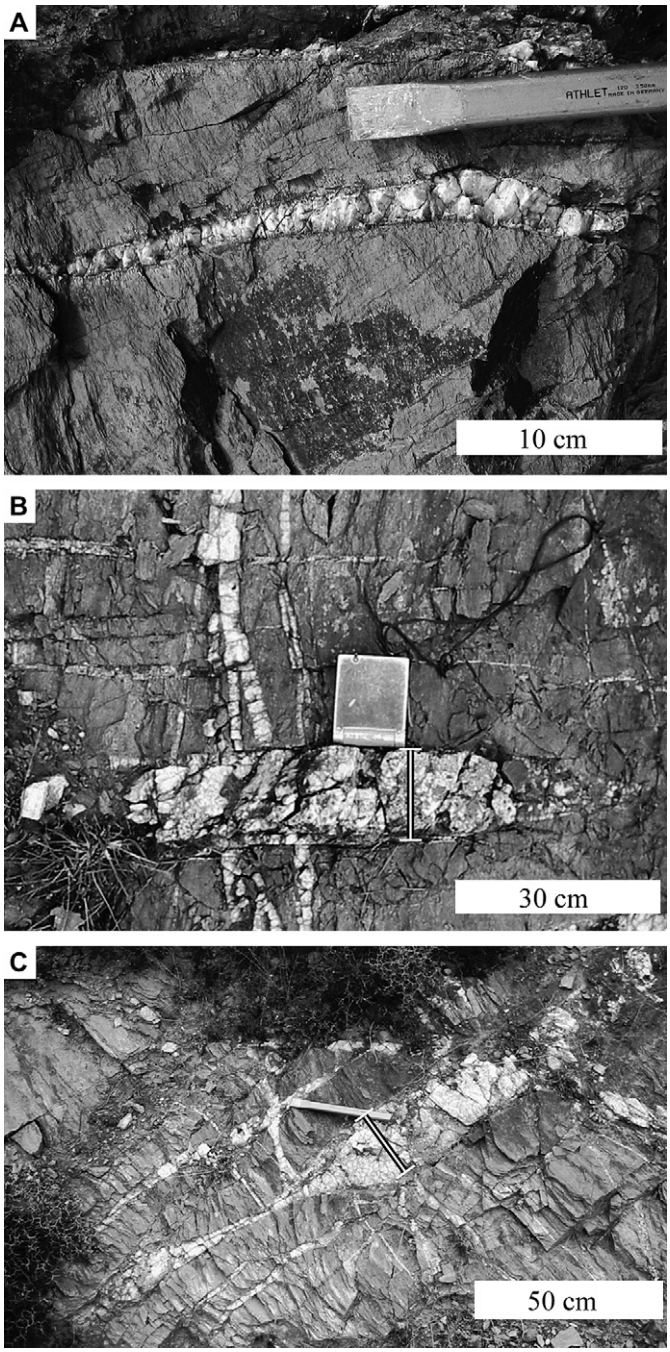

Fig. 2. Discordant quartz veins in the Styra-Ochi Unit selected for analysis. The bars show the sampled profile lines. (a) Lens-shaped vein EN 4a corresponding to vein EN 4. Vein EN 4 got damaged during sampling, before a photograph was taken. (b) The lens-shaped vein EN 38 with a low aspect ratio of about 12 crosscuts pre-existing concordant veins. (c) The irregular shaped vein EN 45 shows swelling and pinching.

$$w = -\sigma'_{\mathrm{n}} \frac{2(1-\nu^2)}{E} L \tag{1}$$

where E denotes the Youngs modulus and ν the Poissons ratio. The state of stress in the material close to the tip of a crack at a distance r under tensile load is proportional to the stress intensity factor K_{I} and to $r^{-1/2}$ (Irwin, 1948, 1956, 1957). The

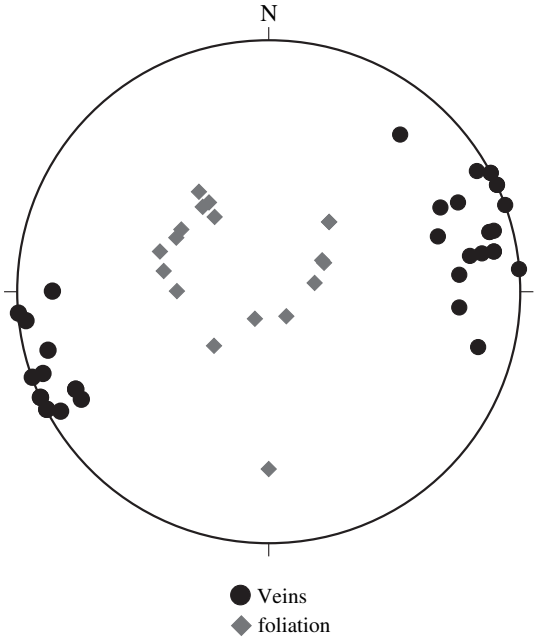

Fig. 3. Stereographic plot (lower hemisphere) of poles to foliation and vein walls at different locations in the Styra-Ochi Unit of South Evia/Greece. The data cover an area of more than 500 km^2.

stress intensity factor K_{I} depends on σ'_{n} and on L (Irwin, 1948, 1956, 1957):

$$K_{\mathrm{I}} = -\sigma'_{\mathrm{n}} \sqrt{\pi \frac{L}{2}} \tag{2}$$

If K_{I} reaches a certain material constant, the fracture toughness K_{IC} (Irwin, 1961), the material fails by initiation of unstable crack propagation:

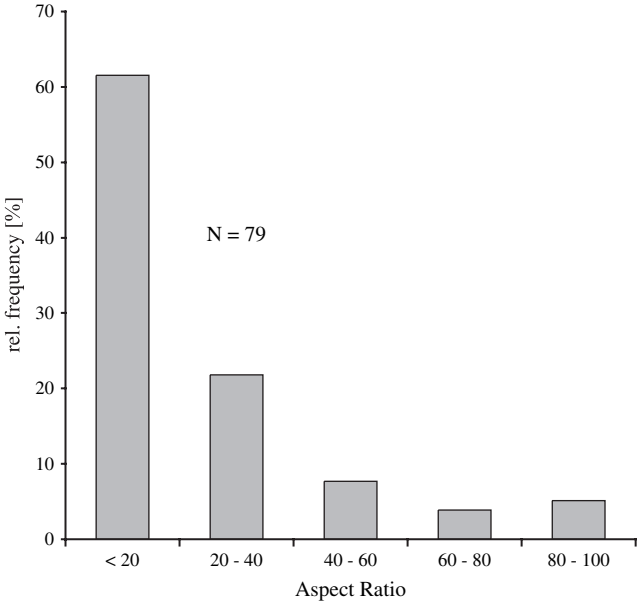

Fig. 4. Histogram showing the frequency distribution of vein aspect ratios. Most veins reveal an aspect ratio of 20 or below.

$$K_{IC} = -\sigma'_{nc}\sqrt{\pi\frac{L}{2}} \tag{3}$$

where σ'_{nc} denotes the critical tensile stress. According to Eqs. (1) and (3), crack opening by linear elastic distortion of the host rock is limited by $\sigma'_n < \sigma'_{nc}$. Implementation of Eq. (3) into Eq. (1) yields a criterion for the maximum possible crack width w_0, sustained by the host rock (Olson, 2003):

$$w_0 = K_{IC}\frac{(1-\nu^2)}{E\sqrt{\frac{\pi}{8}}}\sqrt{L} \tag{4}$$

Eq. (4), solved for K_{IC} (Eq. (5)), can be used to estimate K_{IC} holding for the rock, using the length and aperture data of mineralized veins (Olson, 2003). This approach presumes that the veins formed in response to purely elastic distortion of the host rock and, hence, under LEFM-conditions:

$$K_{IC} = \frac{w_0}{\sqrt{L}}\frac{E\sqrt{\frac{\pi}{8}}}{(1-\nu^2)} \tag{5}$$

Eq. (5) is used to compare the geometry of the discordant veins in the Styra-Ochi Unit to laboratory data for K_{IC} (Atkinson and Meredith, 1987) and to the geometry of single-segment veins described elsewhere. These include veins at Culpepper Quarry (Virginia, USA) and Florence Lake (California, USA; Vermilye and Scholz, 1995), as well as multi-segment dykes at Ship Rock (Delaney and Pollard, 1981) (Fig. 5). The geometry of the Culpepper Quarry and Florence Lake veins is interpreted to result from elastic distortion of the vein walls during cavity formation (Vermilye and Scholz, 1995; Olson, 2003). In contrast, the geometry of magmatic dykes is expected to be strongly influenced by thermal effects due to magmatic heat transfer (e.g. Delaney and Pollard, 1981; DeGraff and Aydin, 1993). Such effects include thermal erosion at the dyke walls (e.g. Delaney and Pollard, 1981) and enhanced plasticity at the dyke tips (e.g. DeGraff and Aydin, 1993), resulting in a marked increase in the fracture toughness due to crack tip blunting (e.g. Anderson, 1995). The geometry of magmatic dykes is expected to be influenced by a number of processes and does hardly reflect a purely elastic deformation of the host rock (e.g. Delaney and Pollard, 1981; Vermilye and Scholz, 1995; Olson, 2003). As K_{IC} is exclusively defined for sharp crack tips stressed at LEFM-conditions, the predictions based on Eq. (5) are referred to as apparent fracture toughness, K^*_{IC}, wherever the values exceed the values for K_{IC} determined in the laboratory (Atkinson and Meredith, 1987). Eq. (5) is solved for the length and aperture data of the discordant veins in the Styra-Ochi Unit using moderate values of $E = 50$ GPa and $\nu = 0.25$ for metamorphic rocks (Turcotte and Schubert, 2002), resulting in values of K^*_{IC} between 3×10^2 and 3×10^3 MPa m$^{1/2}$ (Fig. 5). The K^*_{IC} values derived for the Culpepper Quarry and Florence Lake veins and for the Ship Rock Dyke range between 8 and 25 MPa m$^{1/2}$, and 7.9 and 790 MPa m$^{1/2}$, respectively (Olson, 2003) (Fig. 5). Typical laboratory values of K_{IC} range between 1 and 4 MPa m$^{1/2}$, and in exceptional cases up to 10 MPa m$^{1/2}$ (Atkinson and Meredith, 1987). The calculated apparent fracture toughness, K^*_{IC}, for the discordant veins in the Styra-Ochi Unit exceeds the laboratory K_{IC} data (Atkinson and Meredith, 1987) and the K^*_{IC} of the reference veins (Vermilye and Scholz, 1995; Olson, 2003) by 1–2 orders of magnitudes. The K^*_{IC} of Ship Rock Dyke (Olson, 2003) is exceeded by 70% of the veins. Therefore, the geometry of the lens-shaped veins in southern Evia is in conflict with an origin by purely elastic deformation of the host rock, and is interpreted to reflect a significant contribution of viscous deformation of the host rock during the period of cavity formation.

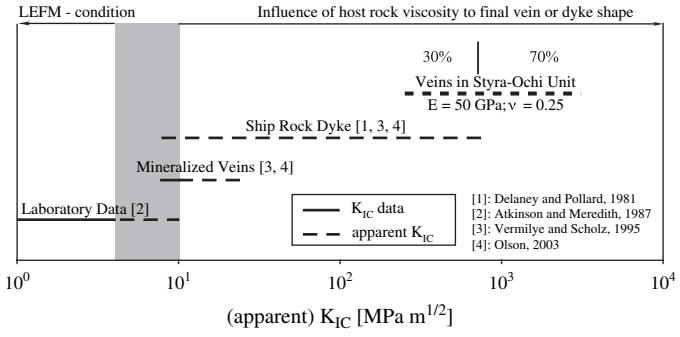

Fig. 5. Comparison of the apparent K_{IC} data derived for the discordant lens-shaped veins in the Styra-Ochi Unit (Eq. (5)) with published data for the magmatic Ship Rock Dyke (Delaney and Pollard, 1981), for Culpepper Quarry and Florence Lake mineralized veins (Vermilye and Scholz, 1995) and with published laboratory data for K_{IC} of rocks (Atkinson and Meredith, 1987).

6. Microfabrics of vein quartz

The quartz microfabrics of 33 discordant veins in the Styra-Ochi Unit of South Evia were investigated by optical microscopy. Three veins, EN 4, EN 38 and EN 45, were selected for a more detailed quantitative analysis of the quartz microfabric along profiles normal to the vein walls (Fig. 2). The dimensions of veins EN 4, EN 38 and EN 45 are $L = 42$ cm, $w = 4.1$ cm; $L = 120$ cm, $w = 10$ cm; and $L = 192$ cm, $w = 21$ cm, respectively. L denotes the vein length and w the maximum aperture.

The veins are sealed by quartz, while other minerals are subordinate and, if present, restricted to a narrow zone close to the vein walls. The microfabrics developed during sealing in EN 4 and EN 45 are representative for the fabrics observed in the vast majority of the 33 microscopically inspected veins. The microfabrics of vein EN 38 show some peculiarities, but are interpreted to reflect the same principal mechanisms of vein sealing as those of the other veins.

The veins EN 38 and EN 45 show the largest aperture of all investigated veins and hence, provide the best spatial resolution along the profiles. While EN 4 and EN 38 represent the most common lens-shape geometry (Fig. 2a, b), EN 45 represents the group of irregular shaped veins, showing some swelling and pinching (Fig. 2c). The comparably small vein EN 4 was chosen in order to explore whether the evolution of the deformation related microfabrics in the vein quartz depends on the size of the vein.

6.1. Vein quartz microfabrics related to sealing

Veins EN 4 and EN 38 are made up almost entirely of quartz. In vein EN 45, subordinate amounts of albite and zoisite are found, restricted to a narrow zone at the vein margin. The present study focuses on the quartz microstructures. The first observation is that inclusion trails parallel to the vein walls (Durney and Ramsay, 1973; Ramsay, 1980; Cox and Etheridge, 1983; Fisher and Byrne, 1990; Fisher and Brantley, 1992; Fisher et al., 1995) are systematically absent in all veins. At the vein margin, the quartz microstructure of EN 4 and EN 45 is characterized by elongate grains with an aspect ratio of 1.5–2 (Figs. 6a, 7a). In contrast, the quartz microstructure at the margins of vein EN 38 is characterized by elongate grains with an aspect ratio of about 3–3.5 (Fig. 8a). In this vein, the majority of the elongate grains appear curved (Fig. 8a, c), their long axis being inclined in opposite directions at both vein margins. The curvature of the grains coincides with a curvature in the crystallographic orientation (Fig. 8a–c).

In all veins, the sealing quartz shows a crystallographic preferred orientation (CPO) of the *c*-axes. In veins EN 4 and EN

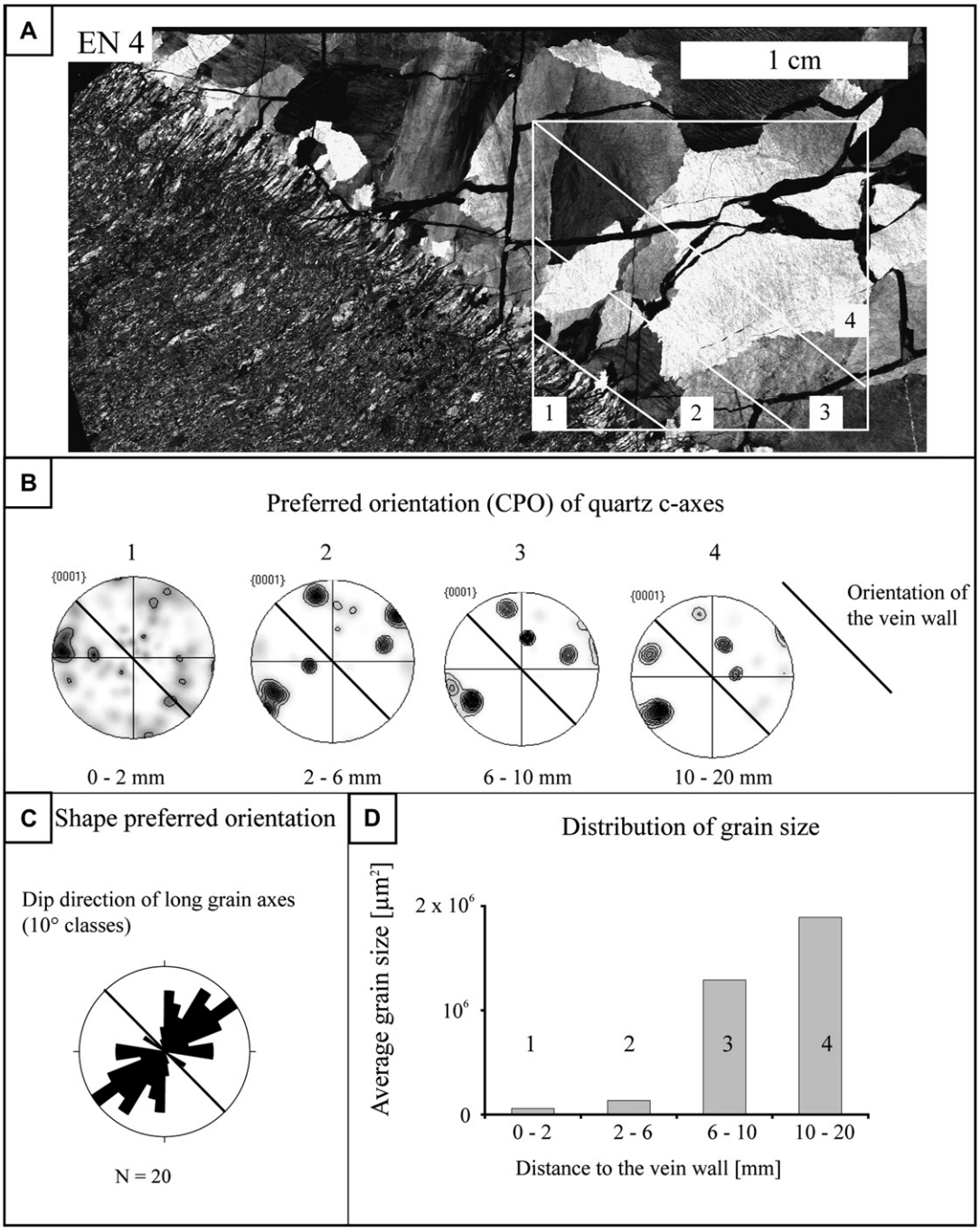

Fig. 6. Quartz microfabrics of vein EN 4, grain shape and orientation data acquired by EBSD. (a) Optical microstructure (thin sections scanned with crossed polarizers). (b) Development of a more pronounced quartz *c*-axes preferred orientation with increasing distance to the vein walls. (c) Shape preferred orientation of the quartz crystals. (d) Increase in quartz grain size with increasing distance to the vein walls.

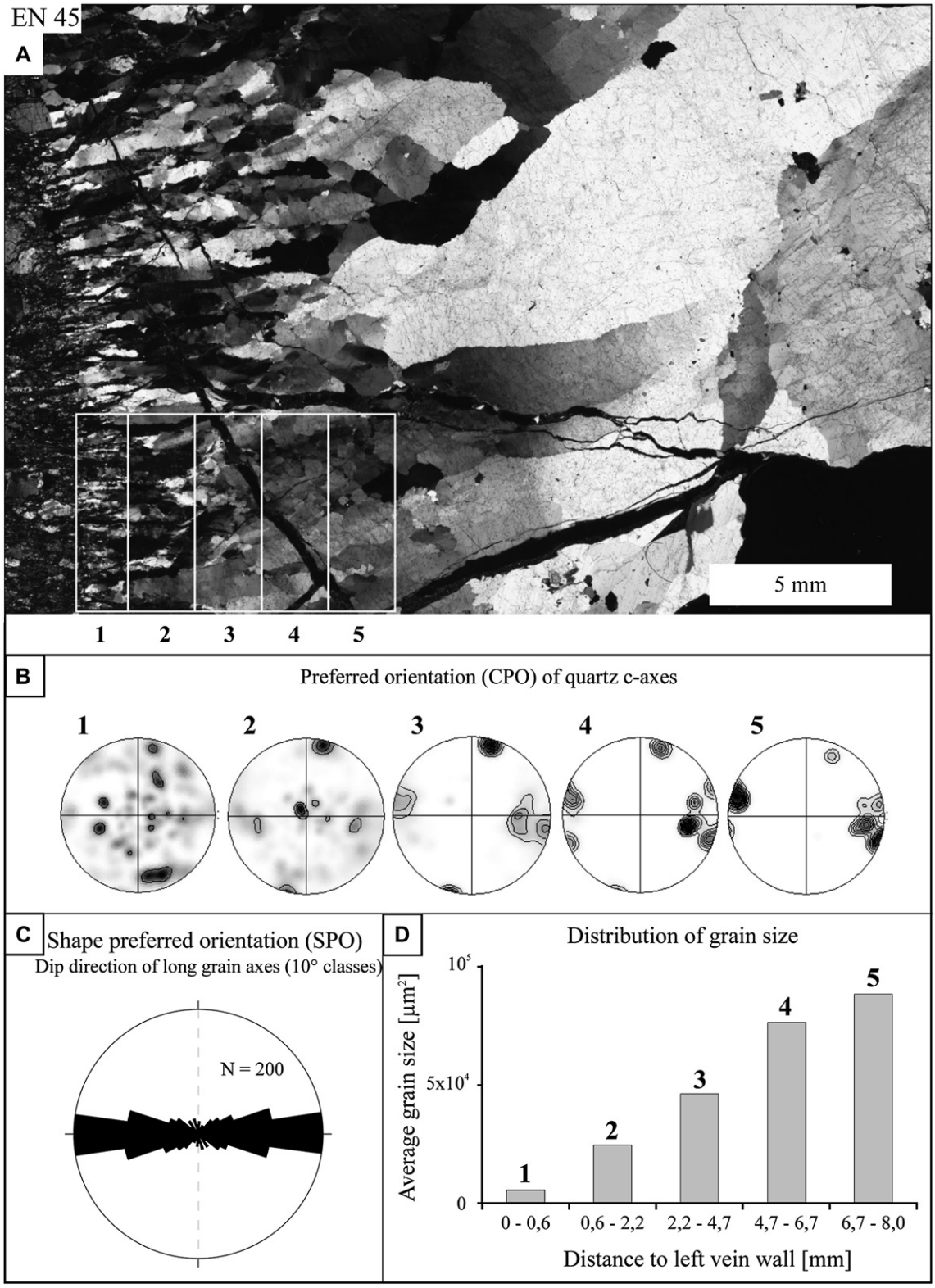

Fig. 7. Quartz microfabrics of vein EN 45, grain shape and orientation data acquired by EBSD. (a) Optical microstructure (thin sections scanned with crossed polarizers). (b) Development of a more pronounced quartz *c*-axes preferred orientation with increasing distance to the vein walls. (c) Shape preferred orientation of the quartz crystals. (d) Increase in quartz grain size with increasing distance to the vein walls.

45, the *c*-axes are preferentially oriented normal to the vein walls (Figs. 6b, 7b), and in vein EN 38, the *c*-axes are oriented at a high angle to the vein walls (Fig. 8b). The CPO of the quartz *c*-axes gets more pronounced over a narrow interval from the vein margin towards the vein centre. Close to the vein margins, the CPO is diffuse with multiple weak maxima (Figs. 6b, 7b, 8b). With increasing distance to the vein walls, the number of maxima decreases and a uniform preferred

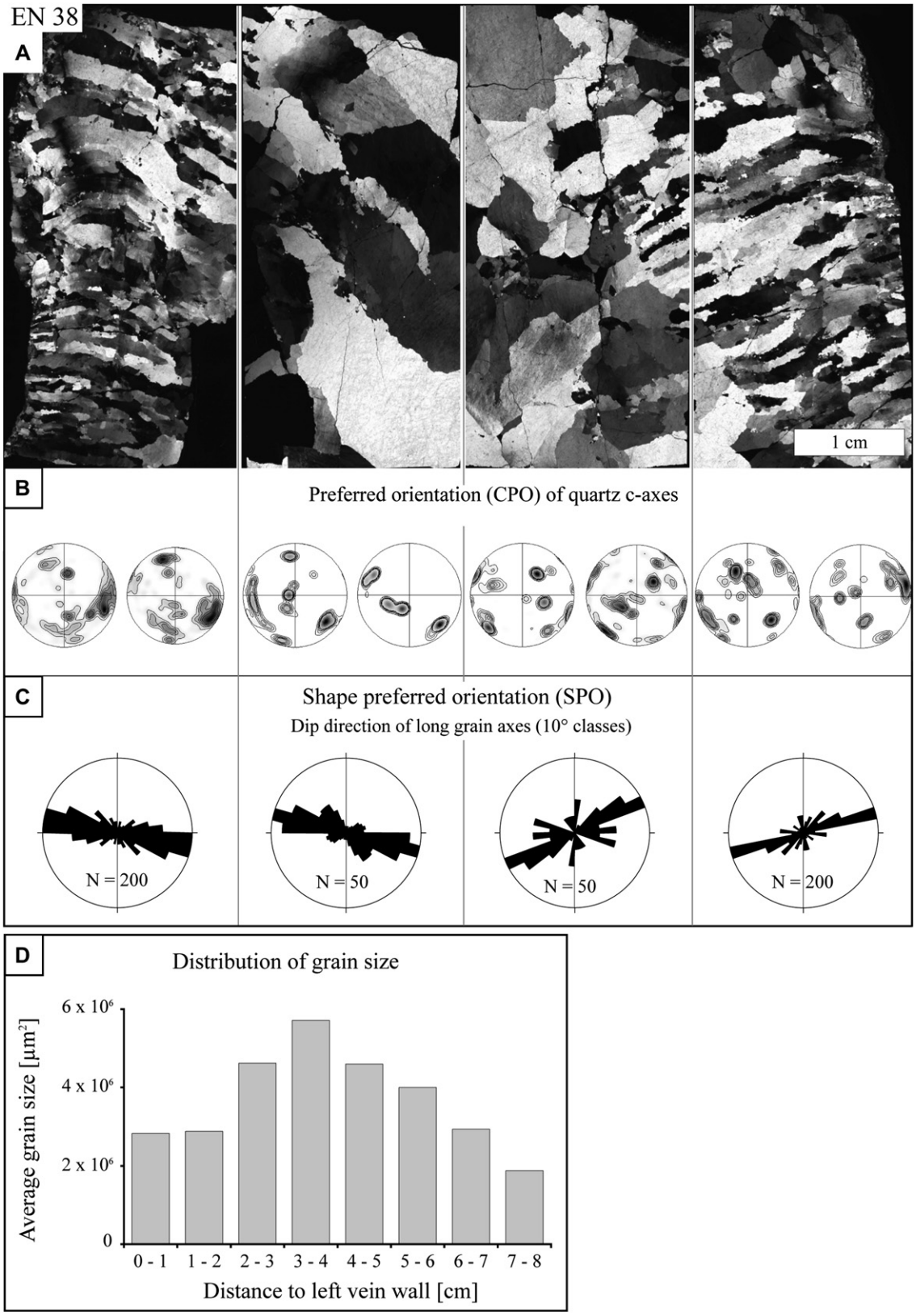

Fig. 8. Quartz microfabrics of vein EN 38, grain shape and orientation data acquired by EBSD. (a) Series of scanned thin sections (crossed polarizers) along a profile across EN 38 presenting the optical microstructure. (b) Development of a more pronounced quartz *c*-axes preferred orientation with increasing distance to the vein walls. (c) Shape preferred orientation of the quartz crystals. (d) Increase in quartz grain size with increasing distance to the vein walls.

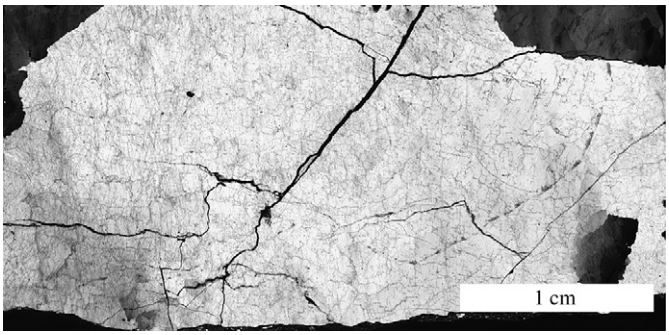

Fig. 9. Centimetre-sized quartz crystals at the centre of vein EN 45. The grains show undulatory extinction. Scanned thin section with crossed polarizers.

orientation of the quartz *c*-axes is developed (Figs. 6b, 7b, 8b). The grains generally display a pronounced shape preferred orientation (SPO), the long axes being oriented parallel to the *c*-axes (Figs. 6c, 7c, 8c). The grain size increases towards the vein centre, resulting in a decrease in the number of grains per cross sectional area (Figs. 6a, d–8a, d). At the vein margins, the grain size ranges between 10 and 100 μm in veins EN 4 and EN 45 (Figs. 6, 7, 10a, 11d), while it is on the millimetre scale in vein EN 38 (Figs. 8a, d, 11a). Close to the centre of the veins, the grains reach several centimetres in diameter (Figs. 8a, d, 9). Residual open vugs bound by crystallographically controlled faces are common and most frequently observed close to the vein centres (Figs. 10d, 11c).

6.2. Vein quartz microfabrics related to deformation

The vein quartz shows microstructures indicative of crystal plastic deformation by dislocation glide, least so in the vicinity of the open vugs (Figs. 10d, 11c). Inhomogeneous deformation is revealed by marked undulatory extinction, deformation bands and deformation lamellae (Figs. 6a, 7a, 8a, 9, 10, 11). Microstructures indicating thermally activated annealing processes comprise subgrains and sutured high angle grain boundaries resulting from strain-induced grain boundary migration (Figs. 10, 11). For the majority of the grains distortion is insignificant and the original grain shape is largely preserved.

6.2.1. Gradients in crystal plastic deformation observed in the optical microscope

According to the predominant microfabrics related to deformation, the veins are subdivided into zones parallel to the vein walls. First, the general characteristics of the microfabrics in each zone are presented. Then, the position of these zones

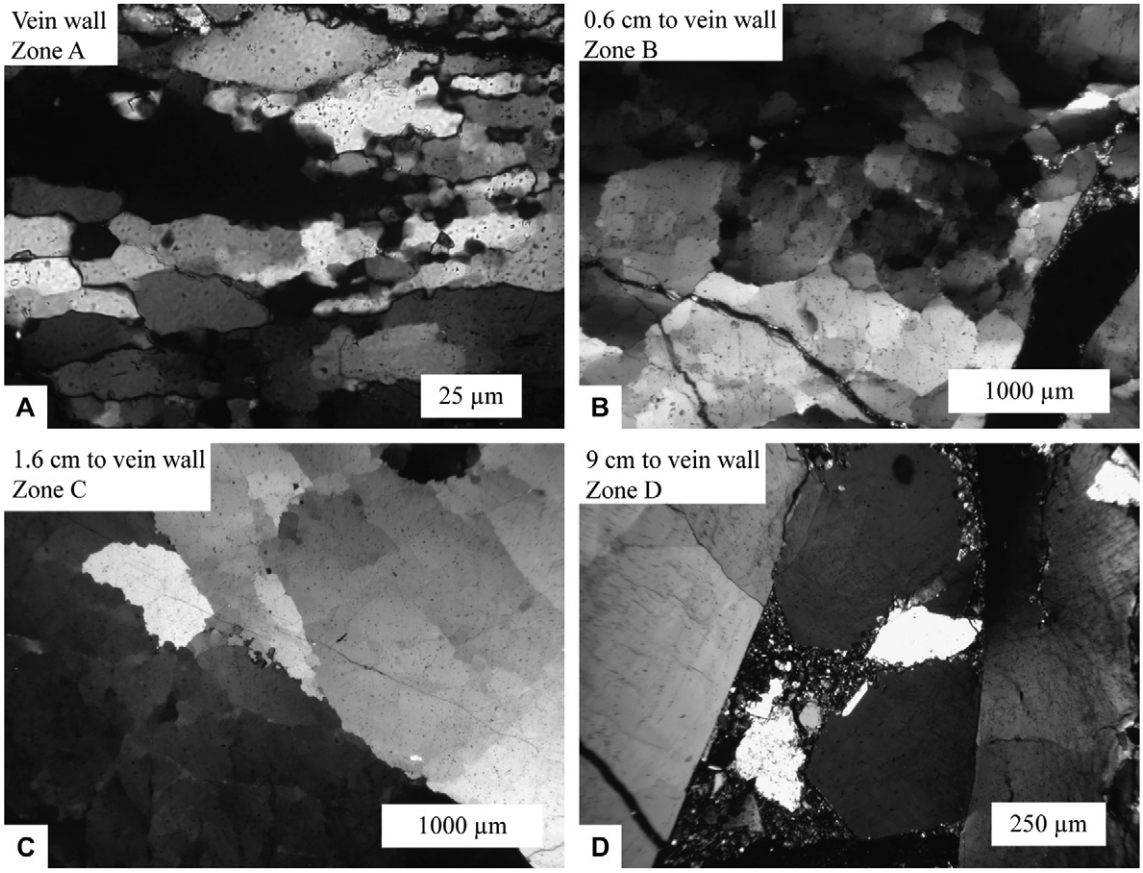

Fig. 10. The quartz microfabrics in vein EN 45 show a decrease in the intensity of crystal plastic deformation with increasing distance to the vein wall. (a) Recrystallized grains close to the vein wall (zone A). (b) Original grain with small subgrains and high misorientation angles at the subgrain boundaries (Zone B). (c) Large subgrains with shape preferred orientation. The misorientation angle at the subgrain boundaries is low. (d) Open vug bound by euhedral facets embedded quartz grains with undulatory extinction. Photomicrographs with crossed polarizers.

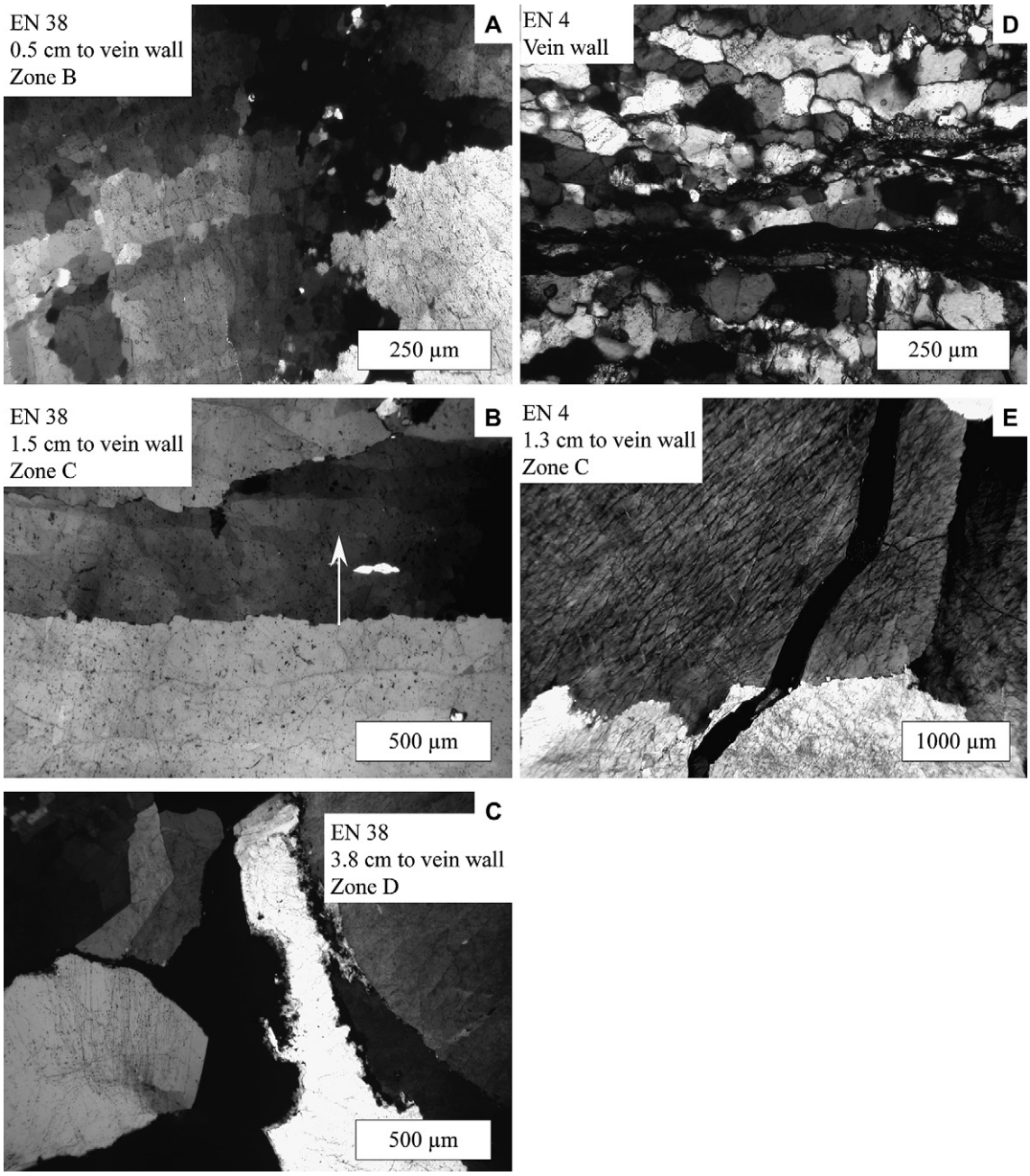

Fig. 11. Microfabrics of quartz in veins EN 38 (a–c) and EN 4 (d, e). (a) Original grains with intense undulatory extinction, small subgrains, and highly sutured high angle boundaries close to the vein wall. Small isometric recrystallized grains are sparse (zone B). (b) Large anisometric subgrains with shape preferred orientation (arrow) (zone C). (c) Open vug bound by euhedral facets embedded in large quartz grains with undulatory extinction. (d) Recrystallized grains at the margin of vein EN 4 (zone A). (e) Large grains in the centre show undulatory extinction and deformation bands. The grain boundaries are sutured. Photomicrographs with crossed polarizers.

and deviations from the standard model are described for each vein.

Zone A represents the outermost part of the veins. Here, recrystallized grains have formed from deformed large original grains (e.g. Hirth and Tullis, 1992) (Figs. 10a, 11d). With increasing distance to the vein walls, the disappearance of recrystallized grains defines the transition from zone A to zone B. In zone B, preserved original grains are intensely polygonized, with small subgrains and high misorientation angles at the subgrain boundaries. The high angle grain boundaries are strongly sutured (Fig. 10b). Towards the vein centre, the misorientation across the subgrain boundaries decreases and the subgrains increase in size. The transition to zone C is marked by the appearance of an SPO of the subgrains, with their long axis aligned parallel to the *c*-axis. In zone C, the high angle grain boundaries are gently sutured

(Fig. 10c, 11b). The innermost zone D is characterized by the absence of subgrains. Instead, the grains show at best a slight undulatory extinction and weakly sutured high angle grain boundaries. Open vugs bound by euhedral facets are common (Figs. 10d, 11c).

Vein EN 45 comprises the zones A–D. In zone A, the diameter of the recrystallized grains ranges between 2.5 and 30 μm (Fig. 10a). The transition to zone B is located at a distance of about 6 mm to the vein wall. Here, the size of the isometric subgrains ranges between 500 and 600 μm (Fig. 10b). The transition to zone C is located at approximately 1.6 cm from the vein wall. Here, the elongate subgrains reach a diameter of up to 2 mm parallel and 0.6 mm normal to the *c*-axis (Fig. 10c). The transition to zone D is poorly defined due to the gradual disappearance of the subgrains at a distance of between 4.8 and 7.7 cm from the vein wall. The first open vugs occur at a distance of 9 cm from the vein wall (Fig. 10d).

Zone A is not discernible in vein EN 38. In this vein, the microfabrics at the vein margin correspond to zone B. Zones C and D are well developed. In the outermost part of zone B a few isolated recrystallized grains occur with a diameter between 10 and 30 μm (Fig. 11a). The microstructure of the original grains is dominated by intense undulatory extinction, small isometric subgrains 15–50 μm in diameter, and strongly sutured high angle grain boundaries (Fig. 11a). The transition to zone C is located at about 1–1.3 cm from the vein wall. The anisometric subgrains measure up to 1 mm in diameter parallel to the *c*-axis, and up to 0.6 mm normal to the *c*-axis (Fig. 11b). The high angle grain boundaries are less sutured compared to zone B (Fig. 11a). The transition into zone D is at approximately 3 cm distance from the vein wall. Open vugs occur close to the vein centre (Fig. 11c).

In vein EN 4, the zones A–C are identified, though their appearance deviates somewhat from the standard model. Zone D is missing. In zone A, the size of the recrystallized grains ranges between 50 and 100 μm (Fig. 11d). The transition to zone B is at about 2 mm distance to the vein wall. Subgrains, comparable to those in EN 38 and EN 45, are absent. Instead, the grains show diffuse deformation bands and elongate subgrains parallel to the *c*-axis. The transition to zone C is located at approximately 5 mm distance to the vein wall. Within zone C, the microstructure is dominated by deformation bands parallel to the *c*-axis and subbasal deformation lamellae (Fig. 11e).

6.2.2. Assessment of gradients in crystal plastic deformation using EBSD maps

EBSD-generated maps provide information on the spatial distribution of the complete crystallographic orientation of the vein quartz. In the following, such maps are used to derive the intracrystalline misorientation gradients, as a function of position within the vein. The misorientation gradients reflect the density of geometrically necessary dislocations (Nicolas and Poirier, 1976) introduced during inhomogeneous crystal plastic deformation.

When crystal plastic deformation is exclusively governed by dislocation glide, the activation of less than five independent glide systems in a single crystal leads to inhomogeneous deformation and distortion of the crystal (Nicolas and Poirier, 1976; Poirier, 1985). This means that the orientation of the indicatrix depends on the position, causing undulatory extinction observed in the polarizing microscope. At moderate temperature and stress conditions, quartz preferentially deforms by glide in the system (0001)<11.0> (basal a-glide) (Hobbs, 1985). Using EBSD maps, the intracrystalline misorientation gradients reflecting the density of geometrically necessary dislocations are quantified as follows.

Colour gradients in the EBSD map in Fig. 12a reflect the degree of misorientation within a single large quartz grain from EN 38 with respect to an arbitrarily chosen reference point. Close to the vein wall, the stereographic plot of the *c*-axis orientations shows considerable dispersion (Fig. 12a), while at some distance to the vein wall the spread of *c*-axis orientation within the same grain is much smaller (Fig. 12a). The observation indicates that the degree of inhomogeneous crystal plastic deformation, i.e. the density of geometrically necessary dislocations, decreases inwards from the vein wall.

For quantification, the angle of misorientation with respect to a reference point is measured along the steepest gradient on EBSD maps (Fig. 12a, b). The misorientation profiles are approximated by a line of best fit (Fig. 12b). The gradient of the line of best fit provides a measure for the intensity of inhomogeneous crystal plastic deformation, and is referred to as the gradient of the misorientation profile, GMP [°/μm] (Fig. 12b). To assess the GMP as a function of position within the veins, EBSD mapping with 10 μm step size was performed on thin sections along a profile normal to the vein walls. The maps were subdivided into subsets. In each subset, several GMPs parallel to the steepest gradient in misorientation were collected. Then, the average GMP is plotted for each subset position within the vein (Fig. 12c). The procedure of GMP determination and creation of a GMP-position plot is illustrated in Fig. 12.

The GMP as a function of position is plotted in Fig. 13 for the three investigated veins. At the vein walls, the GMP is highest and decreases non-linearly by about one order of magnitude towards the vein centre. For the vein EN 38, the pattern is symmetric.

7. Discussion

7.1. Crustal level of fracturing and vein formation

The cracks and the resulting veins postdate the pervasive ductile deformation during HP/LT metamorphism. This is indicated by the fact that the veins crosscut all syn-metamorphic structures of the host rock and that the original vein shape appears to be at best little modified by later deformation. The orientation of the veins is consistent with an origin from tensile cracks and vein formation during crustal extension. This structural record indicates that the veins do not represent deep-seated syn-metamorphic structures, but must have formed during exhumation and cooling.

The vein quartz microstructure records thermally activated annealing processes, which suggests deformation at elevated

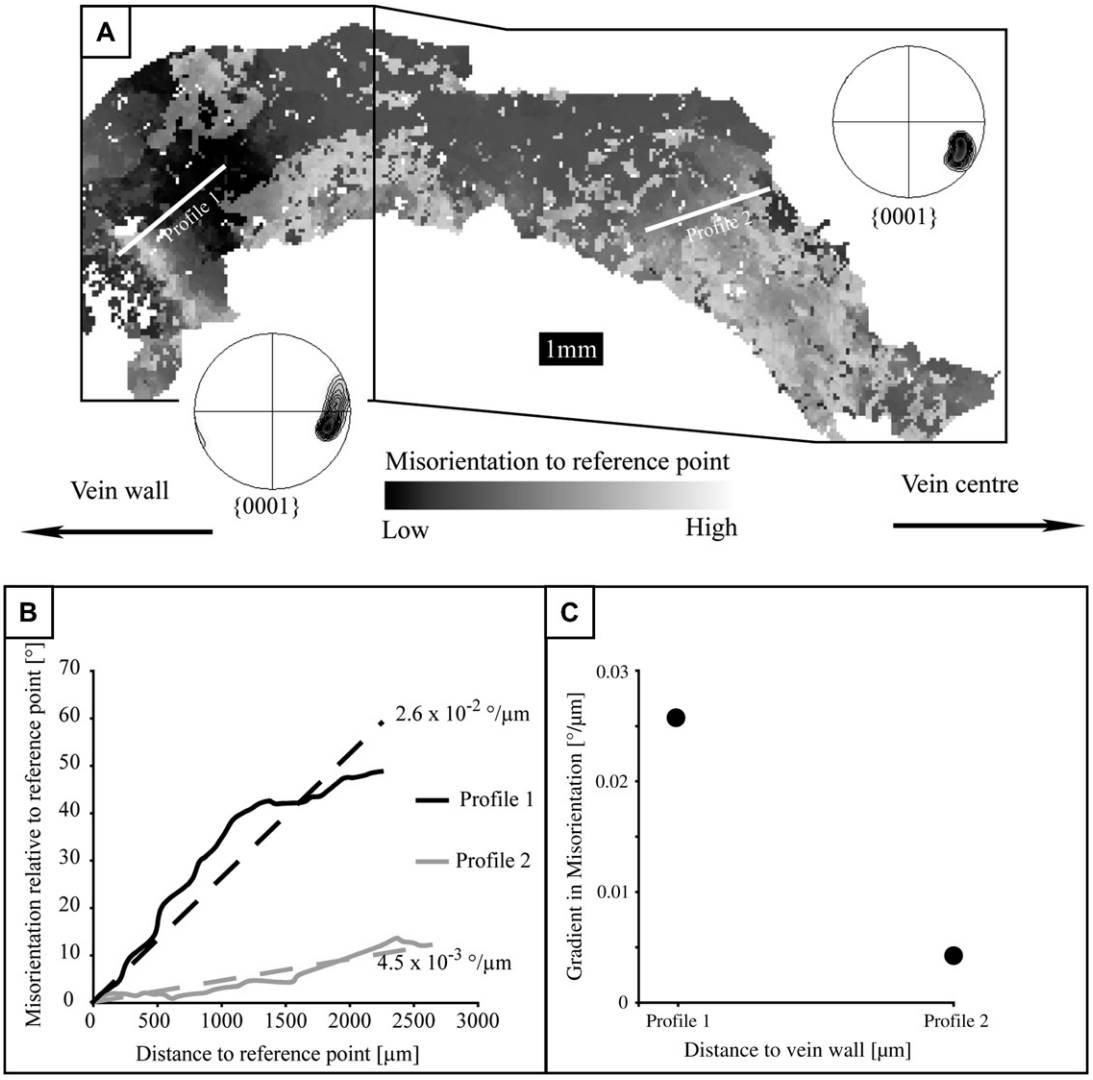

Fig. 12. Principles of the assessment of gradients in crystal plastic deformation. (a) The angle of misorientation with respect to a reference point is measured along the steepest gradient on EBSD maps. (b) The gradient is approximated by a line of best fit, and is referred to as the gradient of the misorientation profile, GMP [°/µm]. (c) The GMP is plotted as a function of the position within the vein.

temperatures. The correlation between thermochronometry and natural quartz microstructures (e.g. Voll, 1976; Dunlap et al., 1997; Stöckhert et al., 1999; Brix et al., 2002), supported by the extrapolation of experimental flow laws to slow geological strain rates (e.g. Hirth et al., 2001), allows one to estimate the temperature prevailing during deformation. Based on these comparisons, the microfabrics point to deformation at temperatures similar to or slightly above 300 °C, hence at a depth just below the crustal scale long-term brittle–ductile transition (Strehlau and Meissner, 1987; Ranalli and Murphy, 1987). As there is no evidence for a complex thermal history (Klein-Helmkamp, 1996) and uniform cooling during exhumation can be assumed, formation of the parent cracks and veins must have taken place at a minimum temperature near to or somewhat above 300 °C. This temperature is expected to allow viscous deformation of the host rock, contributing to crack opening and cavity formation.

7.2. Cavity sealing

The microstructure of the veins provides information on the opening and sealing history (e.g. Durney and Ramsay, 1973; Ramsay, 1980; Cox and Etheridge, 1983; Urai et al., 1991; Fisher and Brantley, 1992; Hilgers and Urai, 2002; Nollet et al., 2005). Two microstructural end-members are considered as diagnostic when addressing the relation between the rates of opening and of sealing:

If the sealing rate exceeds the opening rate, vein formation can get cyclic (Nollet et al., 2005). Incremental widening is followed by complete sealing. The process is referred to as the crack-seal mechanism (Durney and Ramsay, 1973; Ramsay, 1980; Cox and Etheridge, 1983; Fisher and Byrne, 1990; Fisher and Brantley, 1992; Fisher et al., 1995). The indicative microfabrics comprise a fibrous crystal shape,

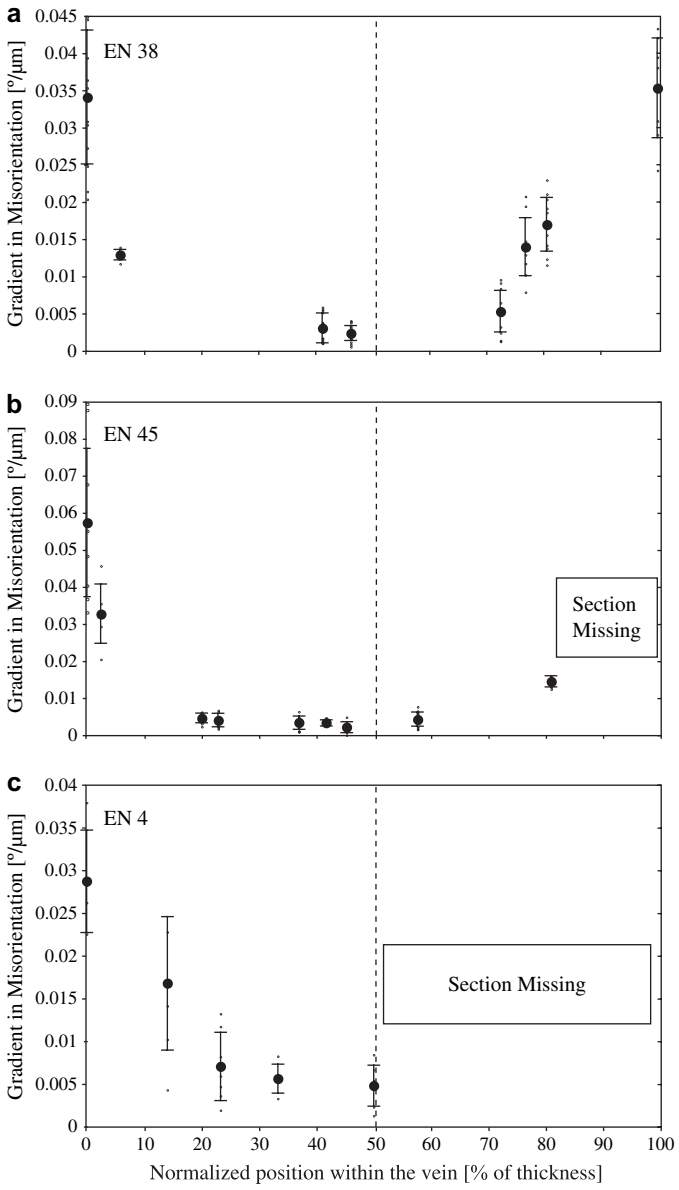

Fig. 13. Plots of the gradients of the misorientation profile (GMP) as a function of the position within the veins. At the vein walls, the GMP is highest and decreases non-linearly by about one order of magnitude towards the vein centres. (a) Vein EN 38; (b) vein EN 45; (c) vein EN 4.

generally without CPO, and narrowly spaced inclusion trails parallel to the vein walls (Durney and Ramsay, 1973; Ramsay, 1980; Cox and Etheridge, 1983; Fisher and Byrne, 1990; Fisher and Brantley, 1992; Fisher et al., 1995). These inclusion trails mark healed cracks. Each trail represents a single increment of opening. Urai et al. (1991) proposed that the grain fibres are detained from development of crystallographic controlled facets by pinning at asperities on the opposite vein wall. Such fibres are capable to track the displacement path during vein widening (Durney and Ramsay, 1973; Ramsay and Huber, 1983; Urai et al., 1991), which can be non-linear. In this case, fibrous crystals can attain a markedly curved shape without a corresponding curvature in the crystallographic orientation (Urai et al., 1991).

If the opening rate exceeds the sealing rate, crystals grow into an open fluid filled cavity (Nollet et al., 2005). In this case, the crystals can develop crystal facets (e.g. Fisher and Byrne, 1990; Fisher and Brantley, 1992; Fisher et al., 1995; Ague, 1994, 1995; Hilgers et al., 2003). The growth of the crystals can be inhibited by growth competition between adjacent grains (Hilgers and Urai, 2002; Hilgers et al., 2003). This leads to a selection of those grains, for which the fastest growth direction is oriented normal to the vein wall (Fisher and Brantley, 1992; Hilgers and Urai, 2002; Hilgers et al., 2003). For quartz, this is the direction parallel to the *c*-axis (Iler, 1979; Fisher and Brantley, 1992). As a consequence of growth competition the number of grains per area is reduced and the grain size increases towards the centre of the vein. Also, a marked preferred orientation of the *c*-axes at a high angle to the vein wall develops (Fisher and Brantley, 1992; Fisher et al., 1995; Hilgers and Urai, 2002; Nollet et al., 2005). Open vugs bound by euhedral crystals represent remnants of the open cavity (Ague, 1995). Such veins, where the crystals grow inwards from the vein walls, are termed syntaxial (Durney and Ramsay, 1973).

The microfabrics of the lens-shaped veins of southern Evia show no discontinuities indicative of multi-stage or cyclic processes of opening and sealing. Instead, the coarse-grained microfabric with elongate or blocky crystals suggests syntaxial crystallization from a fluid phase into a wide open cavity (Yardley, 1986). This is indicated by: (1) the inward increasing grain size (Figs. 6a, d–8a, d): (2) the increasing sharpness of the *c*-axis preferred orientation at a high angle to the vein wall (Figs. 6b–8b); (3) by an SPO with the long axis of the grains oriented parallel to the *c*-axis (Figs. 6c–8c); and (4) residual open vugs bound by crystal faces of large quartz grains at the vein centre (Figs. 10d, 11c) (e.g. Ague, 1995).

An apparent deviation from this simple pattern is observed at the margins of vein EN 38 (Fig. 8). There, the curved grains with a high aspect ratio suggest – on the first glance – that the microstructure may be the result of a cyclic crack-seal process (e.g. Oliver and Bons, 2001). However, characteristic features indicate that the microfabric at the margins of vein EN 38 did also originate by crystallization in an open fluid filled cavity. These features are: (1) a marked inward increase in grain size accompanied by the inward development of a *c*-axis preferred orientation (Fig. 8), with the *c*-axes parallel to the long axes of the grains (Fig. 8b, c), indicates growth competition; (2) the inclusion trails which are characteristic for the crack-seal mechanism (Durney and Ramsay, 1973; Ramsay, 1980) are systematically absent; (3) the curved shape of the grains is accompanied by a corresponding curvature in the crystallographic orientation (Figs. 8b, c); and (4) the long axes of the grains on both vein walls are inclined in opposite directions (Fig. 8a, c). This geometry and the curvature in the crystallographic orientation are not consistent with an origin by displacement-controlled fibrous crystallization (e.g. Urai et al., 1991). Instead, the curvature of the crystals is suspected to result from crystal plastic deformation, although the process is not evident. The coarse anisometric grains close to the vein centre show the same SPO as the grains close to the margins

(Fig. 8), but the evidence of crystal plastic deformation is much less pronounced (Figs 11b, c, 13a). This indicates that the grains at the vein centre must have grown after deformation of the elongate grains at the vein margins.

Based on these observations, the sealing quartz crystallized from the vein walls towards the centre. During progressive sealing, some grains became selected due to impingement. This process is commonly referred to as growth competition and is indicative for sealing of a wide open cavity (e.g. Fisher and Brantley, 1992; Fisher et al., 1995; Hilgers and Urai, 2002). Sealing took place in a single stage, with early grown crystals situated at the vein margins, and lately grown crystals at the vein centre. This holds for the three veins investigated in detail, as well as for all other inspected veins.

7.3. Gradients in crystal plastic deformation indicated by optical microstructure and GMP – position plots

Undulatory extinction of a crystal observed in the polarizing microscope results from the presence of geometrically necessary dislocations (Nicolas and Poirier, 1976). Geometrically necessary dislocations are introduced during inhomogeneous crystal plastic deformation. Their re-arrangement into low-angle grain boundaries indicates syn- or post-kinematic recovery. The size of the subgrains and the misorientation at the subgrain boundaries depend on the density of geometrically necessary dislocations (e.g. Nicolas and Poirier, 1976).

Recrystallization is commonly characterized as either rotation or migration recrystallization (Guillopé and Poirier, 1979; Poirier, 1985). Rotation recrystallization implies the progressive transformation of low-angle grain boundaries into high angle grain boundaries. The increase in misorientation is achieved by progressive incorporation of more and more geometrically necessary dislocations into the grain boundary (Guillopé and Poirier, 1979). Migration recrystallization is indicated by sutured high angle grain boundaries, and is also termed strain-induced grain boundary migration. Depending on whether recrystallization takes place during or after deformation it is referred to as dynamic or static, respectively (Nicolas and Poirier, 1976; Gottstein and Mecking, 1985).

The three selected veins show gradients in the quartz microfabrics related to deformation (Figs. 10, 11, 13), on the optical as well as on the SEM scale. The quartz microstructure of the veins EN 4 and EN 45 reveals abundant small recrystallized grains at the vein margin, and large grains with slight undulatory extinction close to the vein centre (Figs. 9, 10d, 11d, e). In vein EN 38, the vein quartz shows strong undulatory extinction and few small subgrains at the vein margins (Fig. 11a), while the large grains near the vein centre show at best slight undulatory extinction (Figs. 8a, 11c, e). These microstructural gradients are interpreted to reflect a decreasing concentration of geometrically necessary dislocations introduced during inhomogeneous crystal plastic deformation, from the vein margins towards the vein centre, i.e. from early grown to lately grown crystals.

The plots of GMP versus position within the veins show a non-linear decrease in the slope of the gradients. This reflects an inward decrease in the concentration of geometrically necessary dislocations, hence an inward decrease in the degree of inhomogeneous crystal plastic deformation (Fig. 13). The GMP gradients are in accordance with the distinct microstructures observed in the polarizing microscope.

For syntaxial veins sealed by crystallization into a fluid filled cavity, the displacement rate between the fracture walls must have exceeded the sealing rate (Nollet et al., 2005). Two scenarios are possible. (1) Vein sealing commences after instantaneous opening of the cavity, with an aperture corresponding to the width of the final vein. In this case, the crystals grow into a stationary cavity. Distortion of the host rock can be purely elastic. Any crystal plastic deformation of the vein quartz postdates the stage of sealing. (2) Sealing is concomitant with slow opening of the cavity accompanied by crack parallel shortening, which is controlled by viscous deformation of the host rock.

In the second case, single stage syntaxial vein sealing is expected to be a short episode compared to geological timescales. As a first approximation, the sealing process and the concomitant deformation can be considered to be isothermal. The finite strain accumulated during a stage of deformation in a given rheological regime is then controlled by the temperature and the stress history.

In the first scenario, the deformation postdates the sealing stage. All crystals in the vein sealing experience the same stress history at the same temperature. For such a scenario, gradients in the intensity of crystal plastic deformation would require stress concentration due to an inhomogeneous distribution of other minerals in the vein, or systematic differences in the crystallographic orientation yielding a variable Schmid factor (Nicolas and Poirier, 1976), depending on the position within the vein.

First, in vein EN 45, the minor occurrence of rigid zoisite and albite grains at the vein margin may have caused some perturbation in the local stress field. Comparison with vein EN 4, which is a pure quartz vein, does not reveal any contrast in the deformation related microfabrics. Also, the GMP decreases systematically towards the vein centre beyond the marginal zone with subordinate occurrence of other minerals. This rules out an effect of second phase crystals acting as stress concentrators. Second, there is a marked CPO of quartz in all veins, with the *c*-axis oriented perpendicular to the vein wall. This rules out an effect related to crystallographic orientation. Therefore, the systematic decrease in GMP from the vein margins towards the vein centre and the associated changes in the microstructure cannot result from a later stage of deformation affecting the completely sealed vein.

In the second scenario, the gradients in the intensity of crystal plastic deformation are interpreted to result from progressive growth of quartz crystals into a cavity, which is widening by slow viscous creep, while the host rock undergoes some crack parallel shortening (Fig. 14a). In this scenario, the crystals get deformed immediately after their crystallization and the early grown grains have a longer deformation history compared to the lately grown grains (Fig. 14b, c). The time span of deformation, t_d, and hence the accumulated finite strain are reflected by the differing microstructures and in

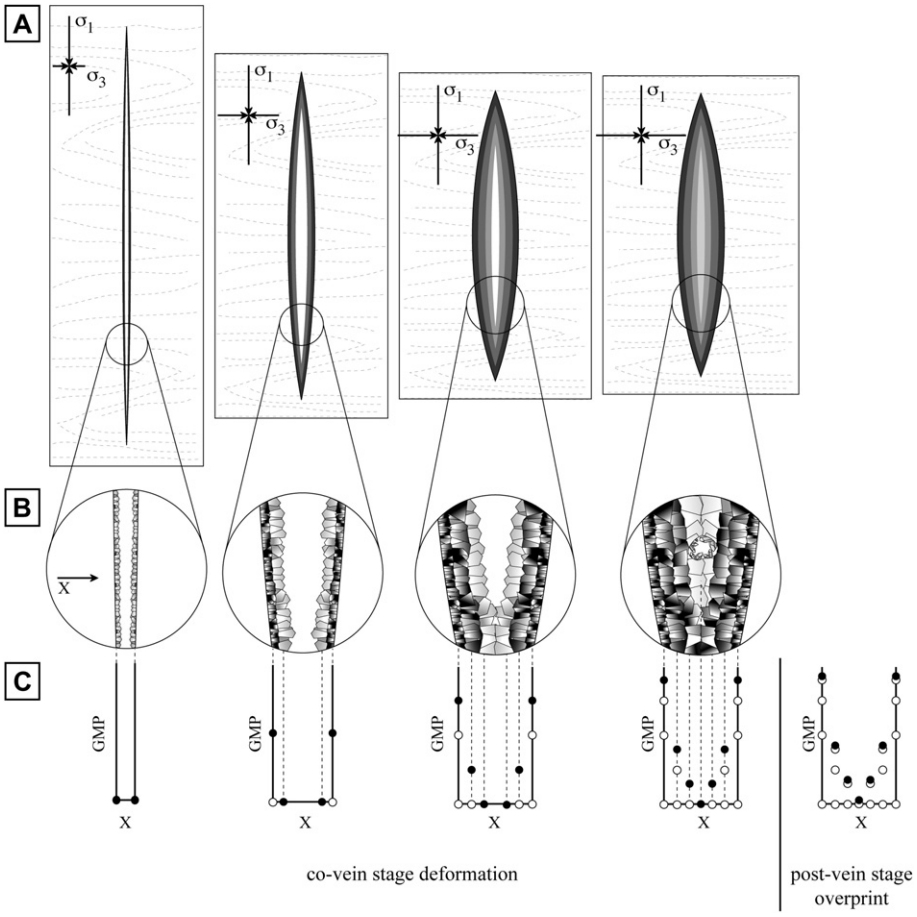

Fig 14. Synoptic diagram illustrating the formation of the veins and the evolution of the vein quartz microfabrics during postseismic stress relaxation. (A) Opening of the fissure by crack parallel shortening of the host rock, concomitant with sealing. (B) Syntaxial crystal growth and progressive deformation during vein formation. (C) Development of the GMP as a function of the position within the vein. The closed symbols denote the actual GMP, the open symbols denote the inferred GMP of previous stages. See text for discussion.

particular the gradient in the concentration of geometrically necessary dislocations. The difference in t_d between two crystals located at the positions x_1 and x_2 along the profiles and crystallized at the time t_1 and t_2, respectively, equals the time interval $\Delta t_d = t_2 - t_1$. The gradients in the intensity of crystal plastic deformation reflect the decrease in t_d with increasing distance to the vein walls (Fig. 14b, c).

The formation of the discordant veins may either take place in an environment of constant deformation of the host rock at low strain rates on geological timescales, or may be controlled by short term stress cycles, presumably induced by seismic activity in the overlying upper crust (Küster and Stöckhert, 1999; Trepmann and Stöckhert, 2001, 2002, 2003). In the first case, the microfabrics of the vein sealing crystals get overprinted by pervasive deformation postdating the sealing stage. In the second case, deformation during the vein sealing stage is a short episode compared to geological timescales. Deformation would then take place with initially high but rapidly decreasing strain rates (Fig. 14) (Trepmann and Stöckhert, 2001, 2002, 2003). In this case, the overprinting of the microfabrics in the completed vein can be less important compared to that during vein sealing (Fig. 14c).

Following the scenario outlined above, the GMP in a given vein quartz crystal results from a portion of inhomogeneous crystal plastic deformation acquired during the stage of progressive cavity opening and sealing, and possibly a portion postdating the vein sealing stage (in the following referred to as co-vein stage and post-vein stage deformation, respectively). The GMP close to the vein walls (GMP_w) would then reflect the entire co-vein deformation and, additionally, the post-vein stage overprint. In contrast, the GMP close to the vein centre (GMP_c) would be expected to result primarily from post-vein stage deformation (Fig. 14).

The percentage of co-vein stage crystal plastic deformation, expressed by $CPD_v[\%]$, is calculated by Eq. (6):

$$CPD_v[\%] = \frac{GMP_w - GMP_c}{GMP_w} \times 100 \qquad (6)$$

The $CPD_v[\%]$ in the veins EN 4, EN 38, and EN 45 are 80–90%, 91–95%, and 95–98%, respectively. The data show that the vast majority of the crystal plastic deformation of the vein quartz is related to co-vein stage deformation, and the post-vein stage overprint is minor. Based on these

considerations, the structural and microstructural features of the discordant veins in the Styra-Ochi Unit in southern Evia are interpreted to reflect a stage of short term and episodic deformation with decreasing strain rates, presumably controlled by seismic activity in the upper crust (Küster and Stöckhert, 1999; Trepmann and Stöckhert, 2001, 2002, 2003; Ellis and Stöckhert, 2004a,b; Ellis et al., 2006). As a first approximation, this process can probably regarded as isothermal, although some thermal perturbation due to advective heat transport by focused fluid flow cannot be excluded.

According to this model, the crystals grown early at the vein margins were subject to higher differential stress and were deformed at a higher strain rates compared to those in the centre of the vein, which have grown at a stage when the coseismically imposed stresses were relaxed and deformation had come to rest (Fig. 14). The microstructural record at the vein margins is therefore proposed to reflect the high stresses and strain rates at the initial stage of crack opening during postseismic creep (Fig. 14). The inward decrease in the intensity of crystal plastic deformation is proposed to reflect the history of stress relaxation (Fig. 14). If so, such characteristic veins in metamorphic rocks can be taken as recorders of the processes and conditions during postseismic stress relaxation in the middle crust, each vein representing a single seismic cycle.

8. Summary and conclusions

The structural and microstructural record of discordant quartz veins in metamorphic rocks of the Styra-Ochi Unit of southern Evia is characterized by the following features:

1. The veins formed in a horizon immediately below the crustal scale brittle–ductile transition, at temperatures of near to or somewhat above 300 °C.
2. The veins formed from arrested cracks. The cracks were widened during minor crack parallel shortening of the host rock, allowing syntaxial growth of crystals into a fluid filled cavity.
3. The aperture to length ratio of the veins exceeds the maximum value feasible for a purely elastic deformation by orders of magnitude. Distributed inelastic deformation of the host rock is required to achieve the final vein shape.

Information on the stage of low strain ductile deformation is exclusively obtained from the microfabrics of the vein sealing quartz and cannot be isolated in the host rock. Systematic gradients in the density of geometrically necessary dislocations in the vein quartz indicate progressive deformation during progressive widening and sealing of the cavity. The intensity of deformation decreases significantly from the margins towards the centre of the veins.

The absence of significant crystal plastic deformation of the crystals in the vein centre shows that deformation of the completely sealed veins is insignificant compared to the deformation during progressive opening and sealing.

The microfabrics of the discordant quartz veins indicate progressive opening and syntaxial sealing in a single event. The early grown crystals at the vein margins record a longer history of deformation at higher initial stresses compared to the crystals grown lately at the vein centre. The microfabrics suggest that stresses were relaxed by creep of the host rock. This is in accordance with the conclusion drawn from linear elastic fracture mechanics considerations that the aperture of the lens-shaped veins cannot result from purely elastic distortion of the host rock. It is proposed that the parental tensile cracks formed as a consequence of rapid coseismic loading to high stress. The subsequent widening of the crack is attributed to the stage of stress relaxation by postseismic creep of the host rock, concomitant with sealing by quartz precipitated from the percolating fluid. The overall finite strain accumulated during the stage of veining is low. Such monogenetic syntaxial veins in metamorphic rocks are proposed to record a single seismic cycle. If so, they provide detailed insight into the conditions and processes active during coseismic loading and postseismic stress relaxation in the middle crust, probably contributing to postseismic strain transients detected by modern geodetic techniques at the surface.

Acknowledgements

Part of this study was funded by the German Science Foundation within the scope of the Collaborative Research Centre 526 ‘‘Rheology of the Earth—from the Upper Crust into the Subduction Zone’’. Discussions with Jörg F. Kalthoff and Andreas Bertram on fracture mechanics helped to develop the ideas and are very much appreciated. Constructive reviews by Tim Little and Steve Miller are gratefully acknowledged.

References

Ague, J.J., 1994. Mass transfer during Barrovian metamorphism of pelites, south-central Connecticut, II, channelized fluid flow and the growth of staurolithe and kyanite. American Journal of Science 294, 1061–1134.

Ague, J.J., 1995. Deep crustal growth of quartz, kyanite and garnet into large-aperture, fluid-filled fractures, north-eastern Conneticut, USA. Journal of Metamorphic Geology 13, 299–314.

Anderson, T.L., 1995. Fracture Mechanics – Fundamentals and Application, second ed. CRC Press, Washington, D.C.

Atkinson, B.K., Meredith, P.G., 1987. Experimental fracture mechanics data. In: Atkinson, B.K. (Ed.), Fracture Mechanics of Rock. Academic Press Limited, pp. 477–525.

Brix, M.R., Stöckhert, B., Seidel, E., Theye, T., Thomson, S.N., Küster, M., 2002. Thermobarometric data from a fossil zircon partial annealing zone in high pressure-low temperature rocks of eastern Crete, Greece. Tectonophysics 349, 309–326.

Cox, S.F., Etheridge, M.A., 1983. Crack-seal fibre growth mechanisms and their significance in the developement of oriented layer silicate microstructure. Tectonophysics 92, 147–170.

DeGraff, J.M., Aydin, A., 1993. Effect of thermal regime on growth increment and spacing of contraction joints in basaltic lava. Journal of Geophysical Research 98, 6411–6430.

Delaney, P.T., Pollard, D.D., 1981. Deformation of host rocks and flow of magma during growth of minette dikes and breccia-bearing intrusions near Ship Rock, New Mexico. U.S. Geological Survey Professional Papers 1202, 1–61.

Dunlap, W.J., Hirth, G., Teyssier, C., 1997. Thermomechanical evolution of a ductile duplex. Tectonics 16, 983–1000.

Durney, D.W., Ramsay, J.G., 1973. Incremental strains measured by syntectonic crystal growth. In: De Jong, K.A., Scholten, R. (Eds.), Gravity and Tectonics. Wiley, New York, pp. 67–96.

Ellis, S., Beavan, J., Eberhardt-Phillips, D., Stöckhert, B., 2006. Simplified models of the Alpine Fault seismic cycle: stress transfer in the mid-crust. Geophysical Journal International 166, 386–402.

Ellis, S., Stöckhert, B., 2004a. Imposed strain localization in the lower crust on seismic timescales. Earth Planets Space 56, 1103–1109.

Ellis, S., Stöckhert, B., 2004b. Elevated stresses and creep rates beneath the brittle–ductile transition caused by seismic faulting in the upper crust. Journal of Geophysical Research 109, B05407.

Faure, M., Bonneau, M., Pons, J., 1991. Ductile deformation and syntectonic granite emplacement during the late Miocene extension of the Aegea (Greece). Bulletin de la Societe Geologique de France, 8ieme Serie 5, 3–11.

Fisher, D.M., Brantley, S.L., 1992. Models of quartz overgrowth and vein formation: deformation and episodic fluid flow in an ancient subduction zone. Journal of Geophysical Research 97, 20,043–20,061.

Fisher, D.M., Brantley, S.L., Everett, M., Dzvonik, J., 1995. Cyclic fluid flow through a regionally extensive fracture network within the Kodiak accretionary prism. Journal of Geophysical Research 100, 12881–12894.

Fisher, D.M., Byrne, T., 1990. The character and distribution of mineralized fractures in the Kodiak Formation, Alaska: implications for the fluid flow in an underthrust sequence. Journal of Geophysical Research 95, 9069–9080.

Freed, A.M., Bürgmann, R., 2004. Evidence of power-law flow in the Mojave desert mantle. Nature 430, 548–551.

Freed, A.M., Bürgmann, R., Calais, E., Freymueller, J., Hreinsdóttir, S., 2006. Implications of deformation following the 2002 Denali, Alaska, earthquake for postseismic relaxation processes and lithospheric rheology. Journal of Geophysical Research 111, doi:10.1029/2005JB003894.

Gautier, P., Brun, J.-P., 1994. Crustal-scale geometry and kinematics of late-orogenic extension in the central Aegean (Cyclades and Evvia Island). Tectonophysics 238, 399–424.

Gottstein, G., Mecking, H., 1985. Recrystallization. In: Wenk, H.R. (Ed.), Preferred Orientation in Deformed Metals and Rocks; an Introduction to Modern Texture Analysis. Academic Press, Orlando, Fl, United States, pp. 183–218.

Guillopé, M., Poirier, J.P., 1979. Dynamic recrystallization during creep of single-crystalline halite; an experimental study. Journal of Geophysical Research 84, 5557–5567.

Hilgers, C., Dilg-Gruschinski, K., Urai, J., 2003. Microstructures grown experimentally from advective supersaturated solution and their implication for natural vein systems. Journal of Geochemical Exploration 78, 221–225.

Hilgers, C., Urai, J., 2002. Experimental study of syntaxial vein growth during lateral fluid flow in transmitted light: first results. Journal of Structural Geology 24, 1029–1043.

Hirth, G., Teyssier, C., Dunlap, W.J., 2001. An evaluation of quartzite flow laws based on comparisons between experimentally and naturally deformed rocks. International Journal of Earth Sciences 90, 77–87.

Hirth, G., Tullis, J., 1992. Dislocation creep regime in quartz aggregates. Journal of Structural Geology 14, 145–159.

Hobbs, B.E., 1985. The geological significance of microfabric analysis. In: Wenk, H.R. (Ed.), Preferred Orientation in Deformed Metals and Rocks: An Introduction to Modern Texture Analysis. Academic Press, Orlando, United States, pp. 463–479.

Iler, R., 1979. The Chemistry of Silica. Wiley-Interscience, New York.

Irwin, G.R., 1948. Fracture Dynamics. Fracturing of Metals. American society for Metals, Cleveland. 147–166.

Irwin, G.R., 1956. Onset of fast crack propagation in high strength steel and aluminium alloys. Sagamore Research Conference Proceedings 2, 289–305.

Irwin, G.R., 1957. Analysis of stresses and strains near the end of a crack traversing a plate. Journal of Applied Mechanics 24, 361–364.

Irwin, G.R., 1961. Plastic zone near a crack and fracture toughness. Sagamore Research Conference Proceedings 4.

Jacobshagen, V., 1986. Geologie von Griechenland. Gebruder Borntraeger, Berlin.

Jolivet, L., Faccenna, C., 2000. Mediterranean extension and the Africa–Eurasia collision. Tectonics 19, 1095–1106.

Klein-Helmkamp, U., 1996. Metamorphose und Exhumierung der niedrigtemperierten Hochdruckmetamorphite der Styra-Ochi-Einheit in Süd-Euböa. Attisch-Kykladisches Kristallin, Griechenland. Ph.D. thesis, Ruhr University Bochum, Germany.

Küster, M., Stöckhert, B., 1999. High differential stress and sublithostatic pore fluid pressure in the ductile regime-microstructural evidence for short-term post-seismic creep in the Sezia Zone, Western Alps. Tectonophysics 303, 263–277.

Le Pichon, X., Angelier, J., 1981. The Aegean Sea. Philosophical Transactions of the Royal Society of London, Series A 300, 357–372.

Lister, G.S., Banga, G., Feenstra, A., 1984. Metamorphic core complexes of Cordilleran type in the Cyclades, Aegean Sea, Greece. Geology 12, 221–225.

Meulenkamp, J.E., Wortel, M.J.R., Van Wamel, W.A., Spakman, W., Hoogerduyn Strating, E., 1988. On the Hellenic subduction zone and the geodynamic evolution of Crete since the late Middle Eocene. Tectonophysics 146, 203–215.

Mullis, J., 1975. Growth conditions of Quartz Crystals from Val d́Illiez (Valais, Switzerland). Schweizerische Mineralogische und Petrographische Mitteilungen 55, 419–429.

Nicolas, A., Poirier, J.P., 1976. Crystalline Plasticity and Solid State Flow in Metamorphic Rocks. Wiley-Interscience, New York, 444 pp.

Nollet, S., Urai, J., Bons, P.D., Hilgers, C., 2005. Numerical simulations of polycrystal growth in veins. Journal of Structural Geology 27, 217–230.

Oliver, N.H.S., Bons, P.D., 2001. Mechanisms of fluid flow and fluid–rock interaction in fossil metamorphic hydrothermal systems inferred from vein–wallrock patterns, geometry and microstructure. Geofluids 1, 137–162.

Olson, J.E., 2003. Sublinear scaling of fracture aperture versus length: an exception or the rule? Journal of Geophysical Research 108.

Poirier, J.-P., 1985. Creep of Crystals – High Temperature Deformation Processes in Metals, Ceramics and Minerals. Cambridge University Press, Cambridge, 260 pp.

Pollard, D.D., Segall, P., 1987. Theoretical displacements and stresses near fractures in rock: with applications to faults, joints, veins, dikes and solution surfaces. In: Atkinson, B.K. (Ed.), Fracture Mechanics of Rock. Academic Press, London, pp. 277–350.

Pollitz, F.F., Wicks, C., Thatcher, W., 2001. Mantle flow beneath a continental strike-slip fault: postseismic deformation after the 1999 Hector Mine earthquake. Science 293, 1814–1818.

Ramsay, J.G., 1980. The crack-seal mechanism of rock deformation. Nature 284, 135–139.

Ramsay, J.G., Huber, M.I., 1983. The Techniques of Modern Structural Geology. In: Strain Analysis, vol. 1. Academic Press, London, 307 pp.

Ranalli, G., Murphy, D.C., 1987. Rheological stratification of the lithosphere. Tectonophysics 132, 281–295.

Rice, J.R., Cleary, M.P., 1976. Some basic stress diffusion solutions for fluid-saturated elastic porous media with compressible constituents. Reviews of Geophysics 14, 227–241.

Scholz, C.H., 1990. The Mechanics of Earthquake and Faulting. Cambridge University Press, Cambridge, 471 pp.

Sneddon, I.N., Elliott, H.A., 1946. The opening of a griffith crack under internal pressure. Quarterly of Applied Mathematics 4, 262–267.

Stöckhert, B., Brix, M.R., Kleinschrodt, R., Hurford, A.J., Wirth, R., 1999. Thermochronometry and microstructures of quartz: a comparison with experimental flow laws and predictions on the temperature of the brittle–plastic transition. Journal of Structural Geology 21, 351–369.

Strehlau, J., Meissner, R., 1987. Estimation of crustal viscosities and shear stresses from an extrapolation of experimental steady state flow data. Geodynamic series 16, 69–87.

Trepmann, C.A., Stöckhert, B., 2001. Mechanical twinning of jadeite; an indication of synseismic loading beneath the brittle-plastic transition. International Journal of Earth Sciences 90, 4–13.

Trepmann, C.A., Stöckhert, B., 2002. Cataclastic deformation of garnet; a record of synseismic loading and postseismic creep. Journal of Structural Geology 24, 1845–1856.

Trepmann, C.A., Stöckhert, B., 2003. Quartz microstructures developed during non-steady state plastic flow at rapidly decaying stress and strain rate. Journal of Structural Geology 25, 2035–2051.

Turcotte, P.L., Schubert, G., 2002. Geodynamics. Cambridge University Press, Cambridge, 456 pp.

Urai, J., Williams, P.F., Roermund, v.H.L.M., 1991. Kinematics of crystal growth in syntectonic fibrous veins. Journal of Structural Geology 13, 823–836.

Vermilye, J.M., Scholz, C.H., 1995. Relations between vein length and aperture. Journal of Structural Geology 238, 423–434.

Voll, G., 1976. Recrystallization of quartz, biotite and feldspars from Erstfeld to the Leventina Nappe, Swiss Alps, and ist geological significance. Schweizerische Mineralogische und Petrographische Mitteilungen 56, 541–647.

Yardley, B., 1986. Fluid migration and veining in the Connemara Schists, Ireland. In: Walther, J.V., Wood, B.J. (Eds.), Fluid–Rock Interactions During Metamorphism. Springer-Verlag, New York, pp. 109–131.